Gamma-Ray Imaging for Void and Corrosion Assessment

Safety and utility of the technology make it appropriate for field application

BY MARIO A.J. MARISCOTTI, FRANK JALINOOS, TERESITA FRIGERIO, MARCELO RUFFOLO, AND PETER THIEBERGER

The use of gamma-rays (γ-rays) for examining concrete samples in the laboratory was first reported by Mullins and Pearson,[1] and the possibility of extracting three-dimensional (3-D) information about reinforcement was pointed out by A.C. Whiffin.[2] Since then, quite a number of papers dealing with the use of electromagnetic radiation in general, such as conventional X-rays, γ-rays from radioactive sources, and radiation from electron accelerators, to examine concrete have been published[3,4]; and the British Standards Institute has issued recommendations for radiography of concrete.[5] However, the systematic commercial application of γ-rays for field inspection, rather than laboratory testing, of concrete structures has been very limited.

In recent years, THASA has developed the reinforced concrete tomography (RCT) method and applied it to hundreds of cases to determine positions and diameters of reinforcing bars with the precision required for condition evaluation of concrete structures.[6,7] This nondestructive testing (NDT) technique uses γ-rays to illuminate sections of beams, columns, and slabs while sensitive films record the transmitted rays. The 3-D reconstruction of the reinforcing bars in the examined sections is obtained from the subsequent analysis of the data recorded in these gammagraphies.

This three-step process is illustrated in Fig. 1: the field work where the gammagraphies are obtained, the data

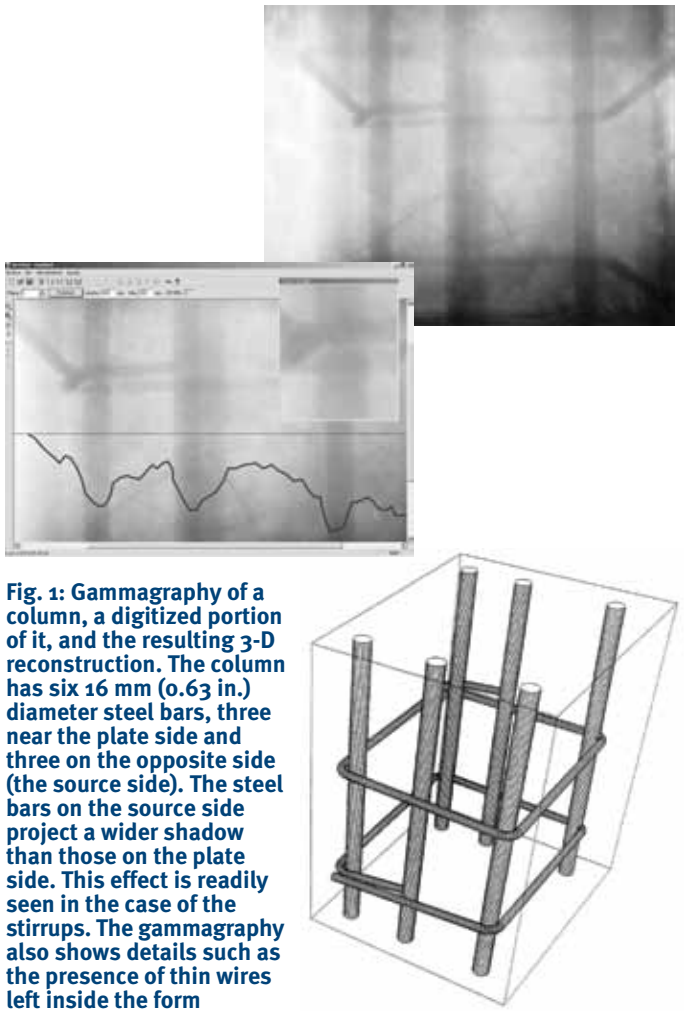

Fig. 1: Gammagraphy of a column, a digitized portion of it, and the resulting 3-D reconstruction. The column has six 16 mm (0.63 in.) diameter steel bars, three near the plate side and three on the opposite side (the source side). The steel bars on the source side project a wider shadow than those on the plate side. This effect is readily seen in the case of the stirrups. The gammagraphy also shows details such as the presence of thin wires left inside the form

Ci online

An additional example application of gamma-ray imaging is summarized with the online version of this article at www.concreteinternational.com

analysis, and the tomographic result. Because gammagraphies, like X-rays, provide images of the interior of the irradiated volume, other characteristics can also be investigated. Of particular importance and current interest is the detection of corrosion in steel elements, such as reinforcing bars, strands, and cables and grout voids in post-tensioning ducts. The "picture" quality of a gammagraphy makes this technique superior to any other current NDT method for addressing these issues.

TOMOGRAPHY METHOD

RCT is similar to computed tomography in the medical field but uses γ-rays from a radioactive source instead of X-rays. In general, tomography of reinforcing bars, ducts, and other elements whose geometrical shape (generally a cylinder) can be assumed requires at least two gammagraphies at different angles, although in some cases only one gammagraphy may suffice.[8] A tomograph comprises two main components: the source assembly and the transmitted radiation detection system.

A γ-ray is a packet of electromagnetic energy (a photon) emitted from the nucleus of a radioactive atom. A radioactive source is characterized by its half-life $T_{1/2}$ and the energy of the photons it emits $E\gamma$ (for sources that emit more than one gamma ray, the energy is expressed as the average $\langle E\gamma \rangle$). Most common sources in NDT are ^{60}Co ($T_{1/2}$ = 5.27 years, $\langle E\gamma \rangle$ = 1250 keV), ^{137}Cs ($T_{1/2}$ = 30.17 years, $E\gamma$ = 662 keV), and ^{192}Ir ($T_{1/2}$ = 73.83 days, $\langle E\gamma \rangle$ = 360 keV).

The latter source, ^{192}Ir, is the least energetic and thus the most portable because it requires the least amount of shielding material to meet radiological protection standards, making it widely used in nondestructive welding inspections.[9] However, the maximum concrete thickness that ^{192}Ir photons can traverse in practical measurement times (about 15 to 30 minutes with conventional films) is only about 300 mm (12 in.). Despite this limitation, most of the studies carried out by THASA, including beams and columns with dimensions in excess of 1 m (3.3 ft), have been performed with a ^{192}Ir source to take advantage of its portability and simplified radiation protection.

In most cases, the study of large volumes is made possible by using the internal source mode,[10] in which the source is placed inside 17 mm (0.7 in.) diameter holes drilled in the structure so that the source-to-plate distance is about 280 mm (11 in.). Because of the relatively high specific activity of ^{192}Ir, a benefit of its short half life, even high intensity sources with about 100 Ci (3.7 TBq) activity fit in small cylindrical volumes of 2 mm (0.08 in.) in diameter and 3 mm (0.12 in.) long, so the disturbance implied by the internal source mode on the structure is actually negligible. Usually the reinforcements are well within 300 mm (12 in.) from one given face of the structure so that, in these cases, the maximum thickness limitation of the ^{192}Ir source is not a problem. However, deeper inspections require a more energetic source or the application of a system where the film is replaced by a γ-ray spectrometer.

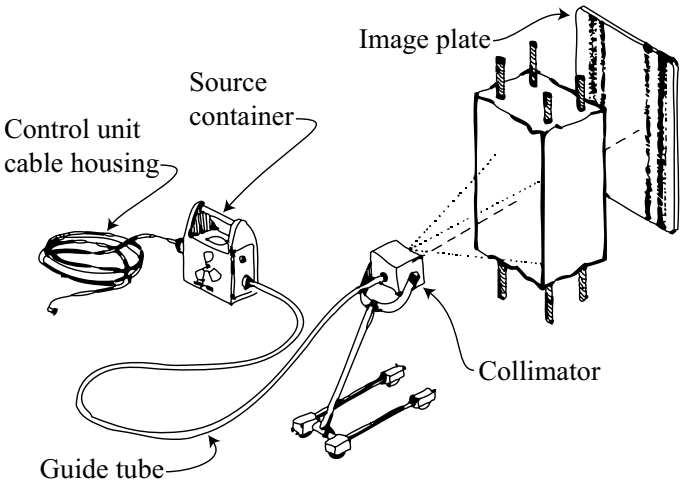

Fig. 2: Schematic representation of a conventional ^{192}Ir source assembly: shielding container (projector), collimator, guide tube, and control unit

Figure 2 shows a simplified conceptual drawing of a conventional ^{192}Ir source assembly. To perform a measurement, the source is displaced to the collimator through the guide tube driven by a control unit comprising a hand crank, a gearbox, a drive cable, and cable housing. The collimator allows radiation to come out only in the direction of the volume to be inspected. In the internal source mode, the collimator is not used and the guide tube is introduced in the hole drilled in the structure.

Until a few years ago, the most common means for detecting the transmitted γ-rays was the traditional 350 x 430 mm (14 x 17 in.) sensitive photographic film. Now, computed radiography (CR) is becoming more popular as prices are increasingly more competitive. A CR system employs reusable image plates that are read with a scanner. CR doesn't require a chemical development process, and the data are immediately available in digital format. Relative to conventional films, CR provides a superior range of detectable γ-ray intensities (by several orders of magnitude) and higher detection efficiency (by factors between 5 and 10), implying a reduction of exposures times (for a given source intensity) or the use of weaker sources (for the same exposure time).

In the RCT method, the plates are supported by special frames[10] that are fixed to the structure to be examined. These frames contain embedded reference objects of a high-density material (such as lead or tungsten), which, under exposure, project fiducial marks (reference points) on the plates. These marks provide precise information on the positions of the source and all the plates involved in the measurement relative to the

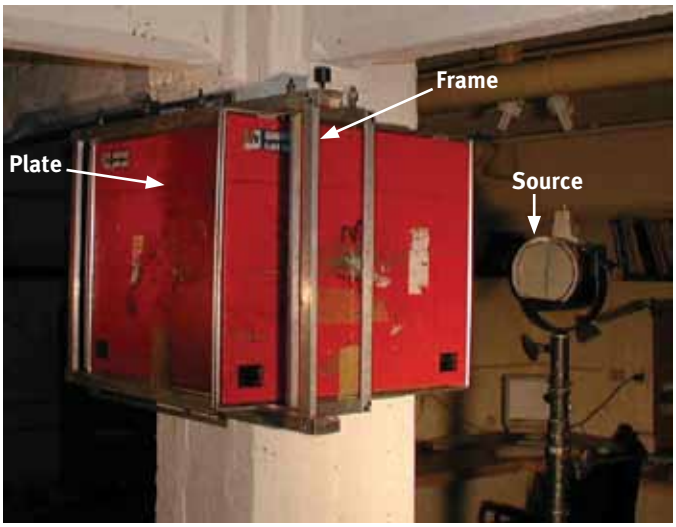

Fig. 3: Plates (in red) are supported by special frames fixed to the structure

Fig. 4: Severely corroded reinforcing bars

structure being inspected, which is essential for accurate 3-D reconstructions.

Figure 3 illustrates one of these arrangements. The plates are inside cassettes (in red); the frame supporting them in this case has two perpendicular planes fixed to a column in such a way that the line intersecting the two planes coincides with one corner of the column. The projector (gray cylinder) is located at a distance (behind the column). The frame carries the high-density reference objects as well as filters that reduce the scattered radiation and improve the image quality. THASA has developed simulation programs that allow the operator to find the optimum filter for each physical configuration.[10,11]

RADIATION PROTECTION

Despite the obvious advantages of this technique, its application is typically limited because of concerns about radiation safety. It's important to note that there is a significant difference (as far as the radiation issue is concerned) between a low energy source such as ^{192}Ir, which is rather simple to shield, and the high-energy X-ray generators that have been used in the past for concrete work. For a 27 Ci (0.99 TBq) ^{192}Ir source as used in most studies, 55 mm (2.2 in.) of tungsten is sufficient to shield the radiation below the dose rate limit allowed for the general public, which is 7.5 μSv per hour, at 1 m (3.3 ft). As a comparison, the dosage of a chest X-ray is between 400 to 1500 μSv, a dental X-ray is 200 to 1500 μSv, and chest tomography is 8000 μSv.[12] The annual dose we receive from natural radiation is 2000 μSv and an intercontinental flight adds about 50 μSv (1 μSv is equivalent to 0.1 mrem).

An external source arrangement such as that shown in Fig. 3, in which the source is in a collimator and radiation impinges on the concrete, produces backscattered radiation, meaning that the operator should stand at least 10 to 15 m (33 to 50 ft) away from the spot. But this requirement is eliminated if additional shielding is applied to reduce the backscattered radiation. The higher efficiency of CR equipment with image plates makes it possible to use much weaker sources, and employing ^{192}Ir greatly diminishes the amount of necessary shielding. It should also be emphasized that for this type of work well-trained and officially licensed operators ensure that all the national and local radiation safety laws and regulations are strictly observed and enforced. It's also worth mentioning that radioactive sources don't induce any radioactivity on the irradiated materials.

The use of ^{192}Ir sources in a systematic way for field inspection of concrete structures is rather new because it was only recently realized that large concrete structures could, in most cases, be investigated with such a low energy source.

EXAMPLE OF CORROSION AND VOID DETECTIONS

Figure 4 shows part of a gammagraphy obtained with a conventional film: a double grid of nominal 8 mm (0.3 in.) diameter bars near the top of a 200 mm (8 in.) thick concrete wall of a refinery tank. The concrete cover is about 400 mm (16 in.) for both grids (distance to nearer wall face). The effect of corrosion in reinforcing bars is to change metal into oxide, the latter being less dense. The absorption of γ-rays, being sensitive to density, will show the loss of metal in a gammagraphy as a change of bar diameter. Because the amount of corrosion varies along the bar length, the phenomenon is seen in a gammagraphy as a change of diameter at different sections.

The gammagraphy of Fig. 4 shows severe corrosion defects, including a section (in the red circle) of reinforcing bar that's disappeared. The following analysis is related to the segment of reinforcing bar highlighted by the red rectangle in Fig. 4. This segment is shown in Fig. 5(a), rotated 90 degrees counterclockwise. A quantitative analysis of the extent of the corrosion in terms of loss of bar section can be done by plotting the position of "edge" pixels along an axis parallel to the bar. Edge pixels define the bar profiles and correspond to the points of maximum slope in the gray level distribution along an axis perpendicular to the bar's main axis for each section. The maximum slope can be found by software methods.[13]

The plots show the edge pixel positions in terms of distance to the "average" of the two values (Fig. 5(b)) and their differences (Fig. 5(c)) along the length of the bars. The data in Fig. 5(c) correspond to the defects in the bar diameter at different sections along its main axis. Defects as large as 2 mm (0.08 in.) are observed. The error of each point is estimated at 0.3 mm (0.01 in.), so defects larger than that can be detected with RCT. A further example is given in Fig. 6. It corresponds to a study carried out on a specimen with corrosion-like embedded defects prepared by the Transport Research Laboratory[14] for the Highways Agency in the U.K. The work was part of a framework contract between Atkins and the Highways Agency[15] to test whether RCT was an appropriate technology to detect corrosion in scissor and dowel bars in deck hinges such as those in hundreds of U.K. bridges.

Measurements were made in August 2007 using a CR system with image plates and a ^{192}Ir irradiation facility provided by GE Inspection Technologies and NDT Services Ltd., respectively.

One of the results of this work[16] is shown in Fig. 6. Figure 6(a) exhibits part of the gammagraphy of one of these bars with a corrosion-like defect on its left profile. The plots (Fig. 6(b)) represent an alternative way to analyze the data for corrosion. Here the photographic

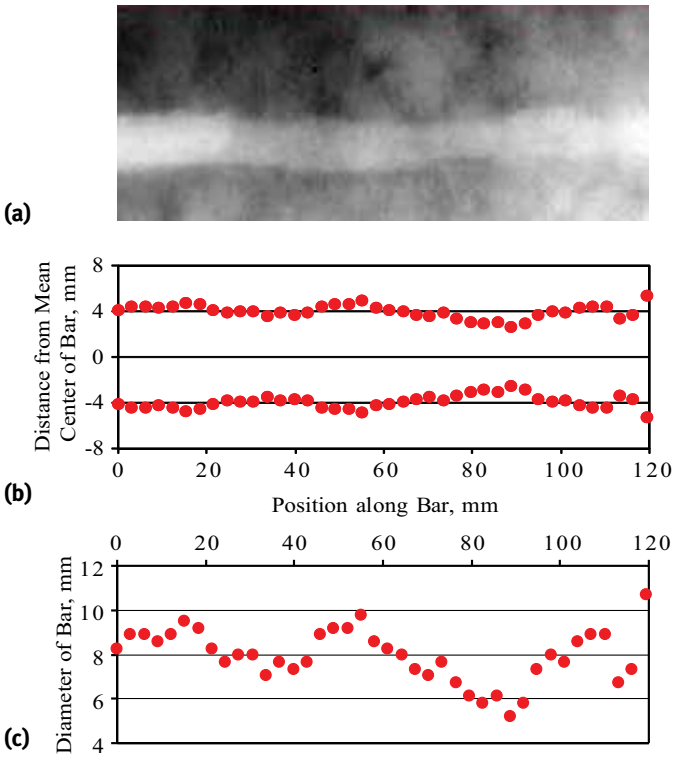

Fig. 5: Analysis of corroded reinforcing bar: (a) gammagraphy of the bar; (b) edge pixel positions in terms of distance to the "mean center" of the bar along bar length; and (c) and diameter of bar (calculated from (b)) (1 mm = 0.0394 in.)

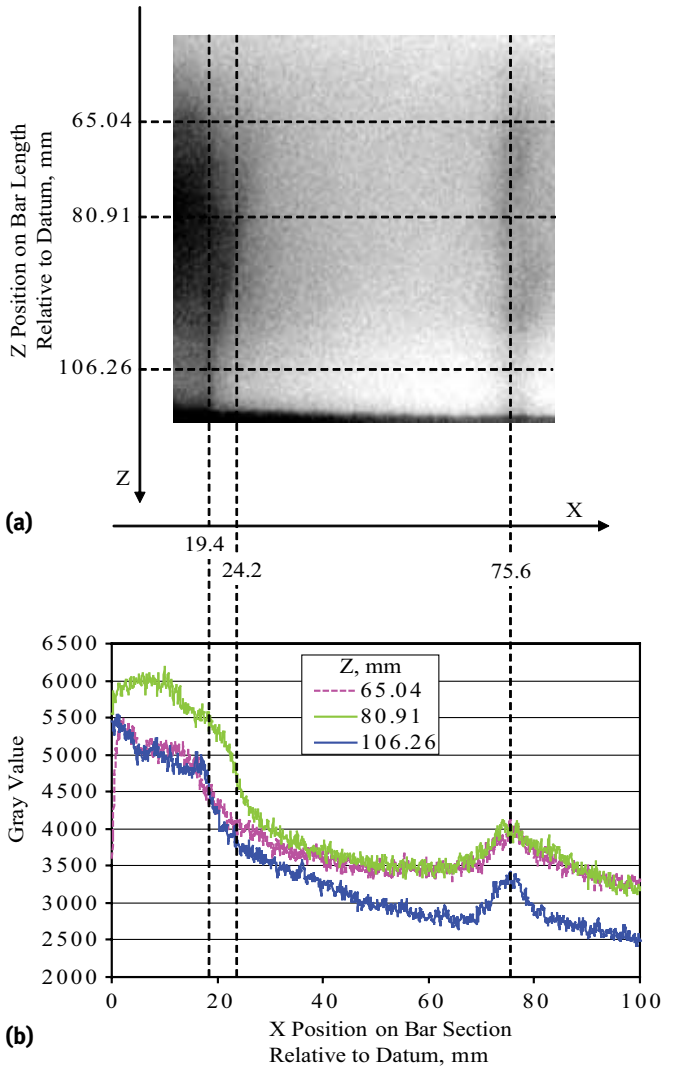

Fig. 6: Analysis of RCT's ability to detect corrosion: (a) part of the gammagraphy of a bar with a corrosion-like defect on its left profile; and (b) the photographic density distributions (pixel gray level values) for reinforcing bar sections indicated in the gammagraphy above. The green data points correspond to the notch seen on the left of the gammagraphy. The notch size is 2.4 +/- 0.2 mm (0.09 +/- 0.01 in.) (1 mm = 0.0394 in.)

density of each pixel along a line that cuts the reinforcing bar's projected image on the plate in a direction perpendicular to the bar axis is plotted as a function of distance along the same line from an arbitrary origin, at three different bar sections. The light green data points correspond to the notch seen on the left of the gammagraphy. The difference at the point of maximum slope with the data in magenta and blue is 4.8 mm (0.19 in.), which corresponds to an actual notch size in the bar of 2.4 +/- 0.2 mm (0.09 +/- 0.01 in.).

SUMMARY AND ADDITIONAL APPLICATION

Gamma-ray imaging is a very useful tool for detecting corrosion and voids in reinforced concrete structures. The risk of radiation exposure is minimal, especially compared with other typical exposure sources. An example of the use of γ-ray imaging for inspection of PT girders is provided in an appendix to this article. The appendix can be viewed at the end of the electronic version of this article available at **www.concreteinternational.com**.

REFERENCES

1. Mullins, L., and Pearson, H.M., "The X-Ray Examination of Concrete," *Civil Engineering and Public Works Review*, London, UK, 1949, pp. 256-258.

2. Whiffin, A.C., "Locating Steel Reinforcing Bars in Concrete Slab," *The Engineer*, London, UK, 1954, pp. 887-888.

3. Malhotra, V.M., *Testing Hardened Concrete: Nondestructive Methods*, ACI Monograph No. 9, Iowa State University Press, 1976, pp. 109-131.

4. McCann, D.M., and Forde, M.C., "Review of NDT Methods in the Assessment of Concrete and Masonry Structures," *NDT&E International*, V. 34, No. 2, Mar. 2001, pp. 71-84.

5. British Standards Institute, "Testing Concrete, Recommendations for Radiography of Concrete," BS 1881: Part 205, 1986, pp. 1-12.

6. Frigerio, T.; Mariscotti, M.A.J.; Ruffolo, M.; and Thieberger, P., "Development and Application of Computed Tomography in the Inspection of Reinforced Concrete," *Insight*, V. 46, No. 12, Dec. 2004, pp. 742-745.

7. Mariscotti, M.A.J., and Husni, R., "Reinforced Concrete Tomography and its Application to Bridge Assessment," *NDE Conference on Civil Engineering*, I. Al-Qadi and G. Washer, eds., St. Louis, MO, 2006, pp. 349-356.

8. Mariscotti, M.A.J., Process for determining the internal three-dimensional structure of a body opaque to visible light by means of radiations from a single source, specially suitable for reinforced concrete parts, U.S. Patent No. 5,828,723.

9. Halmshaw, R., "The Use and Scope of Iridium 192 for the Radiography of Steel," *British Journal of Applied Physics*, V. 5, No. 7, July 1954, pp. 238-242.

10. Thieberger, P.; Mariscotti, M.A.J.; Ruffolo, M.D.; and Frigerio, T., Method and arrangement for improving tomographic determinations, particularly suitable for inspection of steel reinforcement bars in concrete structures, International Patent WO 2008/060398.

11. Thieberger, P.; Mariscotti, M.A.J.; and Ruffolo, M., "Simulation Program for Reinforced Concrete Tomography with Gamma-Rays," *NDE Conference on Civil Engineering*, I. Al-Qadi and G. Washer, eds., St. Louis, MO, 2006, pp. 332-339.

12. "Radiological Protection for Medical Exposure to Ionizing Radiation," Safety Standards Series No. RS-G-1.5, International Atomic Energy Agency, Vienna, Austria, 2002, 75 pp.

13. Mariscotti M.A.J., "A Method for Automatic Identification of Peaks in the Presence of Background and its Application to Spectrum Analysis," *Nuclear Instruments and Methods*, V. 50, No. 2, May 1967, pp. 309-320.

14. Badr, A.; McKenzie, M.; Scorey, V.; and Hassan, K., "Production of Reinforced Concrete Specimens with Embedded Defects," UPR/IE/215/06, Framework Contract 3/359, TRL Limited, Dec. 2006.

15. "ATK—Gamma Ray Tomography for Reinforced Concrete," SSR Framework Contract—Task Ref: 152 (387), Atkins Highways & Transportation, 2006, pp. 1-23.

16. Mariscotti, M.A.J.; Thieberger, P.; Frigerio, T.; Mariscotti, F.; and Ruffolo, M., "Detection of Defects in Reinforced Concrete Hinge and Half Joint Specimens," THASA Technical Note *NT 13-07*, 2007, pp. 1-16.

Selected for reader interest by the editors.

ACI member **Mario A.J. Mariscotti** is CEO of THASA, Buenos Aires, Argentina, and President of THASA US, Brookhaven, NY. In 1992, he founded THASA (www.thasa.com), a company dedicated to the development and application of nuclear technologies in civil engineering such as gamma-ray tomography of concrete structures, detection of steel reinforcement corrosion, honeycombing and grouting defects in post-tensioned girders, and the use of neutrons for atomic element identification in concrete. He received a PhD in nuclear physics and has carried out basic research in several international laboratories, mainly at Brookhaven National Laboratory.

Frank Jalinoos is the Program Manager of the Federal Highway Administration (FHWA) Nondestructive Evaluation (NDE) Center, McLean, VA. He has more than 25 years of experience in civil NDE, instrumentation, and ground imaging. His main area of research includes NDE imaging of both concrete and steel highway infrastructure elements. Other areas of interest include pavement NDE, structural health monitoring, and subsurface geophysical investigations.

Teresita Frigerio is a Professor of secondary education physics and has studied computing science. She has been THASA's Software Developer since 2001.

Marcelo D. Ruffolo has been in charge of THASA's R&D Laboratory since 2001 and is Chief Field Operator. He was a Research Assistant at the Radiobiological Department of the Argentine Atomic Energy Commission and is currently in his last year as a student of medical physics.

Peter Thieberger is a Senior Physicist at Brookhaven National Laboratory. He is well known for his contributions in nuclear spectroscopy and instrumentation and for his developments in particle accelerators. As a THASA Partner, he has contributed ideas for improvements in measurement technique and has developed simulation software useful in planning inspections and interpreting results.

GAMMA-RAY MEASUREMENTS IN A PT GIRDER

An inspection of a post-tensioned girder was carried out at the Zárate Bridge in Argentina. This cable-stayed road and railway bridge was built between 1972 and 1978 and refurbished in 1998. Designed by the Italian engineer Fabrizio de Miranda, the Zárate Bridge crosses the Paraná River between the Buenos Aires and Entre Ríos provinces (Fig. A).

The bridge has a suspended length of 550 m (1804 ft), with a main span of 330 m (1083 ft). The bridge pylons are 110 m (361 ft) high, and the deck is 2.6 m (8.5 ft) thick. The road link has four lanes. The main span is 50 m (164 ft) above the water level of the Paraná River, which allows the passage of very large ships. One of the 300 mm (12 in.) thick girders at the west end of the bridge (to the left in Fig. A) has a total of six grouted ducts. The ducts were inspected for voids in the grout using gamma-rays (γ-rays) from a 93 Ci ^{192}Ir source.

Gammagraphies were taken in the positions indicated in Fig. B using plates with conventional films. As a reference, the distance between Plates 1 and 2 is 700 mm (28 in.). Figure C provides an overview of the 15, 350 x 430 mm (14 x 17 in.) gammagraphies obtained in this study, and Fig. D exhibits enlargements of four of these gammagraphies. Gammagraphy 1 shows a severe void in the grouting of the upper duct. In gammagraphy 2, this defect is still evident but less marked than in 1. Also, minor voids in the upper part of ducts in gammagraphies 8 and 13 are discernible.

Figure E shows the photographic density along the vertical dotted line in Fig. D (plate 1). The coordinate Z goes from the bottom up in the gammagraphy as shown in Fig. D. “Valleys” in this plot at Z ~ 100 mm (4 in.) and 220 mm (8.7 in.) correspond to the lower and upper ducts, respectively, and the peak at ~ 270 mm (10.6 in.) corresponds to the void in the grouting of the upper duct. Computation results using mathematical relationships describing the experimental setup were carried out with the results shown in solid and dotted lines in Fig. E. The solid line corresponds to a calculation assuming a void in the upper duct and the dotted line to a calculation assuming no voids. The input parameters were: a) known absorption coefficient (0.03 cm^2/g [0.015 ft^2/lb]) for ^{192}Ir γ-rays; b) source to plate distance, 600 mm (23.6 in.); c) girder thickness, 300 mm (12 in.); d) concrete density, 2.5 g/cm^3 (156 lb/ft^3); e) ducts positioned at the center of the girder; f) ducts’ internal diameter, 72 mm (2.8 in.); and g) cable diameter, 52 mm (2 in.). Points e, f, and g were obtained independently by the tomographic analysis of the plates. The only adjustable parameters in this calculation were the grouting density in the upper duct (0.3

g/cm^3 [18.7 lb/ft^3]) and the density of both cables (set to 3.5 g/cm^3 (218 lb/ft^3). The grouting density in the lower duct was assumed equal to that of concrete. For comparison, the result of a calculation assuming no void is shown in Fig. E with dotted line (in this case the density in the upper duct was taken equal to that of the concrete instead of 0.3 g/cm^3 (18.7 lb/ft^3).

The following conclusions can be drawn from these results:

1) At the maximum photographic density, the depth of the void is a little more than 60 mm (2.4 in.), equivalent to about 50 mm (2 in.) of air as the fitted density in this volume is 0.3 g/cm^3 (18.7 lb/ft^3);

2) Considering that the maximum density of a cable composed of bundles of steel wire is about 80% steel density, the fitted density of 3.5 g/cm^3 (218 lb/ft^3) indicates that the cable's packing factor is about 55%;

3) The difference between calculated and measured values at Z ~ 250 mm (9.8 in.) corresponds to a steel thickness deficiency in the top wires of the upper duct of up to 7 mm (0.3 in.), which may be an indication of corrosion. In the other gammagraphies shown in Fig. D, no steel thickness deficiency signaling corrosion has been observed beyond the measurement uncertainty of 0.3 mm (0.01 in).

Fig. A: The Zárate Bridge

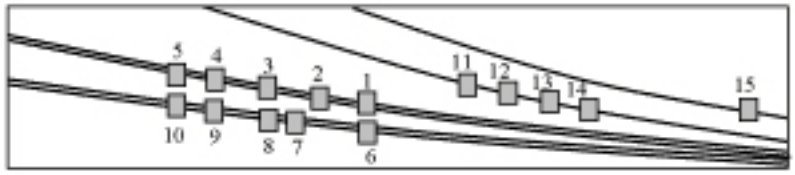

Fig. B: Schematic location of the gammagraphies taken in this work

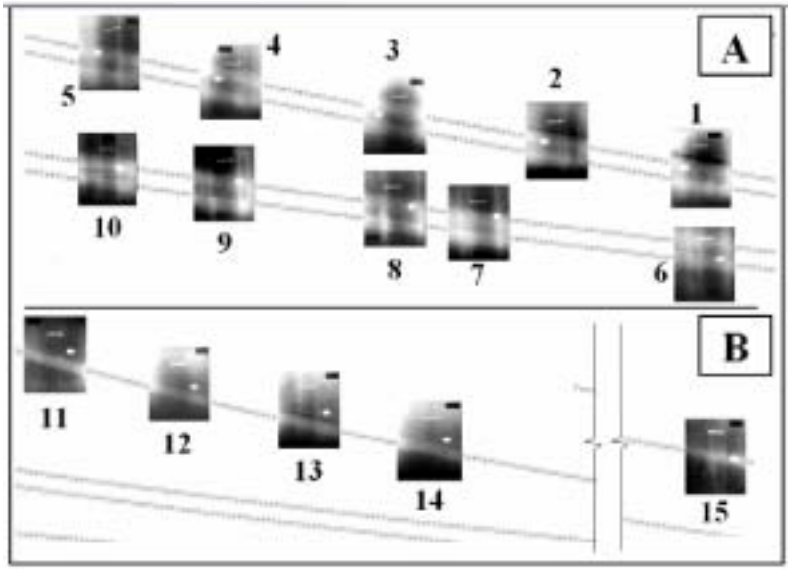

Fig. C: Overview of the gammagraphies obtained in this work. Frame B corresponds to the right part of the girder (see Fig. B). As discussed in the text, gammagraphies 1, 2, 8, and 13 exhibit defective grouting, most notably in 1

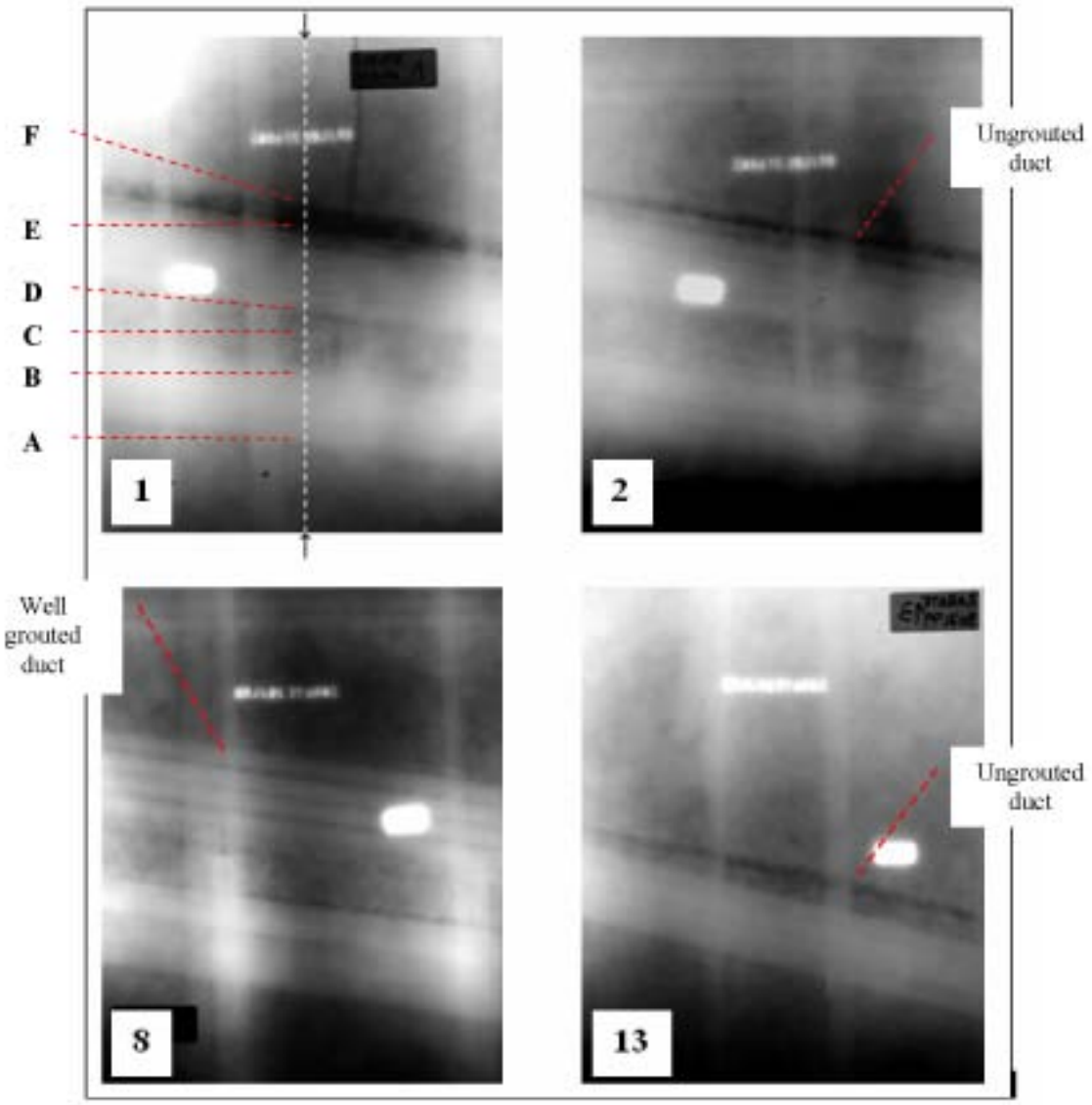

Fig. D: Illustrative examples of the measurements carried out in Zárate Bridge. Gammagraphy 1 shows a severe void in the grouting of the upper duct. In 2, this defect is still present but diminished. In the upper duct in 8, the different bundles of wires can be appreciated, and in both the lower duct of 8 and upper duct of 13 thin black lines show slight voids. These gammagraphies also show stirrups as white vertical bands. The cable and duct diameters are approximately 51 mm (2 in.) and 76 mm (3 in.), respectively

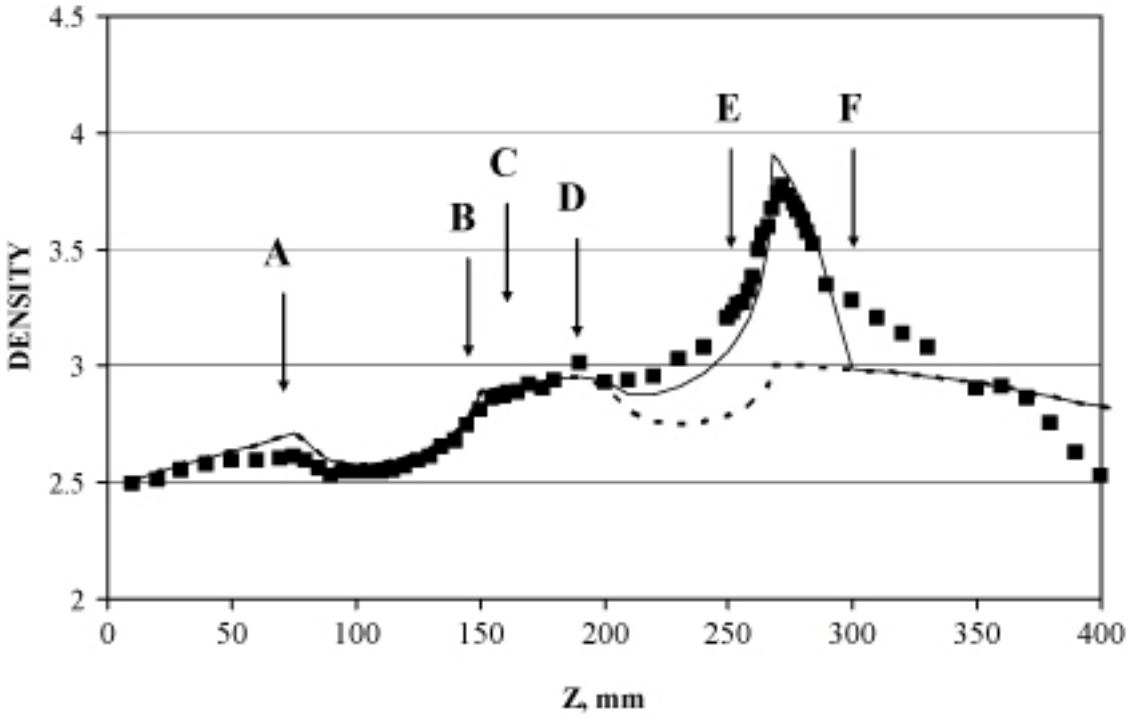

Fig. E: Photographic density along vertical line on plate 1 in Fig. D. Points are measured data, the solid line shows the results of the calculation with defects, and the dotted line shows the results of the calculation without defects. A-B: lower cable; A-C: lower duct; D-E: upper cable; D-F: upper duct (see Fig. D)